Microwave Review
July 2024, Vol. 30, No. 1, pp. 87-91
DOI: 10.18485/mtts_mr.2024.30.1.12

A Dual-Band Second-order Planar BPF Using Aperture Coupling for C/Ku-Band Applications

Rashmita Mishra[1], Ajit Kumar Patro[2], Kailash Chandra Rout[3]

Abstract – **The design and analysis of a dual-band second-order bandpass filter (DBSO-BPF) utilizing the aperture coupling technique for C-and Ku-band application is presented in the proposed work. The design method is applied as a straightforward way to create two transmission poles and the second-order BPF for the C-and Ku-band frequency range. In the first stage, the standard microstrip feed's input impedance is determined and fixed at 50 ohms. Then, a cuboid shape is dug in the middle of the structure; it is connected to the ground of the structure. A copper strip covers the ground part, and two copper strips or stubs are directly connected with the 50-ohm feed line on the top of the structure. In addition, a cuboid and two stubs were used to form two poles and resonant frequencies in two-cavity resonators, developing a dual-band second-order BPF. As a result, it enhanced the impedance bandwidth. Furthermore, the filter's impedance bandwidth and other properties are maintained mainly by the space between two stubs. The design structure is simulated and then analyzed, and the outcomes are confirmed through experimentation. The simulation findings are compared and validated with the experimental results of the filter characteristics.**

Keywords – **Aperture coupling; Broadband; Dual-band; Insertion loss; Impedance matching; Second order.**

I. INTRODUCTION

The development of next-generation communication networks has increased the demand for bandpass filtering systems that can handle massive amounts of data or information. In order to satisfy many standards, bandpass filters (BPFs) are crucial parts of RF/microwave systems [1]. Numerous researchers have proposed various methods for synthesizing and designing BPFs.

In current scenarios, advancements with varying levels of sophistication have been offered for using BPFs. In addition, heavy and bulky filters with specific band-pass sections are used most frequently in space applications; size and mass minimization are crucial in these situations. High-performance, lightweight, and compact filters are discussed in this work. The small C-/Ku-band broadband waveguide filters for satellite applications are proposed in this study.

The most critical conditions to be met simultaneously in both C- and Ku-band filters are i) the in-band loss, ii) the wide spurious free stop-band, and iii) the mass and volume reduction. From the perspectives of compactness and band-pass, TM resonators are a viable option since they enable a reduction in filter length of up to 75% in comparison to traditional filters based on TE mode cavities [2]– [6] while maintaining high Q-factor values (>4000). Such resonators enable the fulfilment of mass, volume, and loss requirements; however, they cannot satisfy the project's vast stop-band need. Multi-aperture irises rather than single-aperture irises have been suggested in [7] as a way to widen the stop band. Unfortunately, this project still needs more refinement. Recently, a few works have been reported [8]-[12], such as narrow BPF along with low profile using FSS structure [8], vertically integrated substrate integrated suspended line BPF [9], SIW-based BPF [10], multilayer-dual-band BPF [11], and ultra-compact SIW-BPF [12].

Article history: Received February 13, 2024; Accepted March 18, 2024.

[1]Rashmita Mishra, is with the Ph.D research scholar in the Dept. of Electronic and communication Engineering, GIET University, Gunupur, Odisha, India-765022, E-mail: rasmita.mishra@giet.edu.

[2]Ajit Kumar Patro and [3]Kailash Chandra Raut are with the faculty in the Dept. of Electronic and communication Engineering, GIET University, Gunupur, Odisha, India-765022, E-mail: [2]ajitpatro@giet.edu; [3]kailash.rout@gmail.com

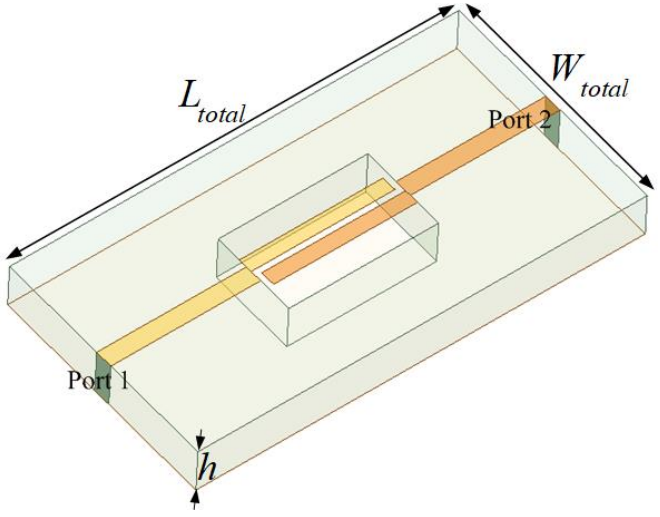

Fig. 1. 3D view of the proposed bandpass filter

This work proposes the broadband bandpass filter (BPF) with enhanced stopband performance, low profile, compact size, and good selectivity for both C and Ku band applications. The proposed simple BPF has enhanced the bandwidth using an aperture coupling technique. Two stubs play a significant role in order to improve the impedance bandwidth. In addition, the proposed BPF is designed, simulated, fabricated, and experimentally verified. To the best of the authors' knowledge, the proposed filter performs better while being smaller and more compact than those described in the literature [13]-[14]. RT/duroid 5880 (ε_r = 2.2, tanδ = 0.0004, and thickness = 1.524 mm) was utilized as the substrate material for the design and modelling investigations of the filters. Ansys HFSS 2020R2 software was used to simulate and optimize filter parameters. The results of the practical environmental tests (thermal, sine, and random vibration) on both filters show that the proposed bandpass

filter concepts are appropriate for broadband broadcasting communication satellites. At the end, a comparison table is provided to compare the similar types of works that have been reported.

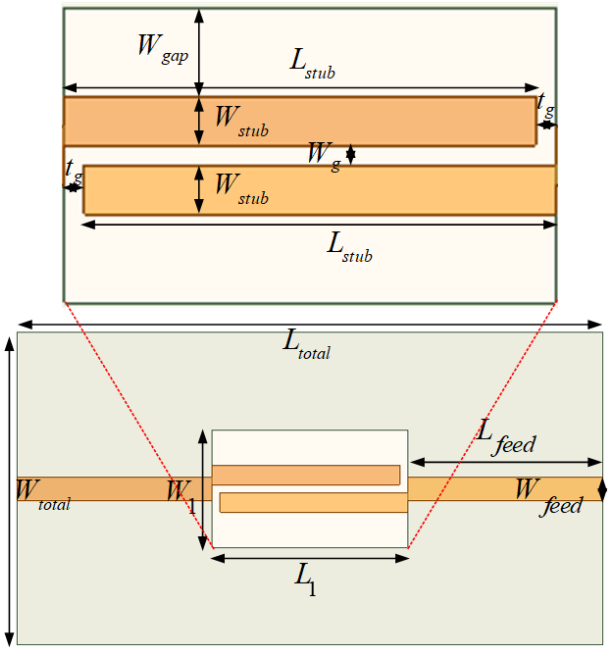

Fig. 2. Geometric of proposed DBSO-BPF (front view)

II. C AND KU-BANDPASS FILTER DESIGN AND RESULTS

The three-dimensional (3D) and top views of the proposed dual-band second-order BPF (DBSO-BPF) are illustrated in Fig. 1 and 2, respectively. The bottom part is a fully ground plane. The proposed DBSO-BPF geometry uses a Rogers 5880 (tm) substrate (15mm x 8 mm x 1.524 mm) having a relative permittivity (ε_r) of 2.2 and loss tangent ($tan\delta$) of 0.0004**.** The proposed dual-band second-order band pass filter for C- and Ku-band is achieved by utilizing the aperture coupling concept and TM mode cavity resonators in microstrip planar technology. As previously reported, a few similar types of work have been detailed in references [15]-[17]. Nevertheless, some improvement is required for this work. Hence, this work was started in order to improve the filter characteristics and compact size. An extensive spurious-free range can be obtained using the aperture coupling effect, and a compact low-loss construction can be obtained using a TM single-mode cavity.

The design method is used straightforwardly to implement two transmission poles and the second-order BPF for the C- and Ku-band frequency range. In an early stage, two standard microstrip feeds as an input impedance of two ports (port-1 and 2) are determined and used in the DBSO-BPF, along with the fixed impedance at 50 ohms. A cuboid shape is dug in the middle of the structure; it is directly connected by radiating to the ground plane of the structure. Then, a copper strip covers the ground part, and two copper strips or stubs are directly connected with the 50-ohm feed line on the top of the structure. In addition, a cuboid and two stubs were used to form two poles and resonant frequencies in two-cavity resonators, developing a dual-band second-order BPF. As a result, it enhanced the impedance bandwidth. Furthermore, the filter's impedance bandwidth and other properties are maintained mainly by the space between two stubs. All the simulations were carried out using Ansys HFSS 2020R2 electromagnetic software.

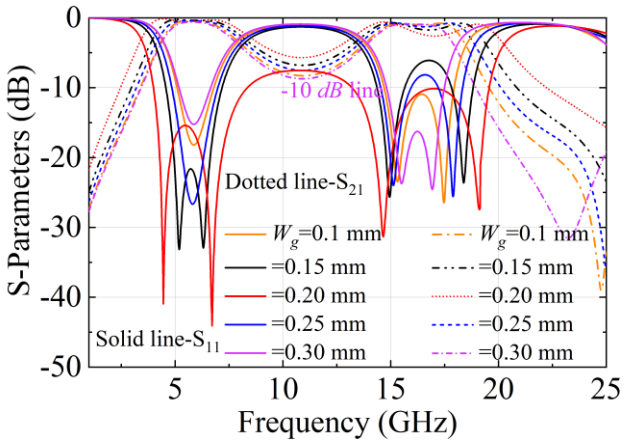

Fig. 3. Reflection coefficient effect on W_g

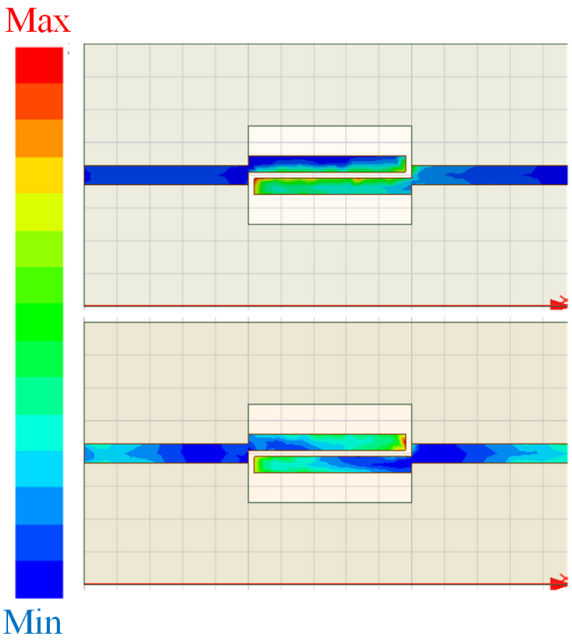

Fig. 4. Electric field distribution (top) at 6 GHz and 16.25 GHz (center frequency)

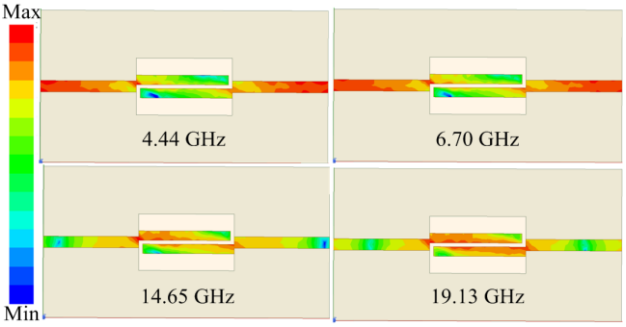

Fig. 5. Surface current distribution at different frequencies

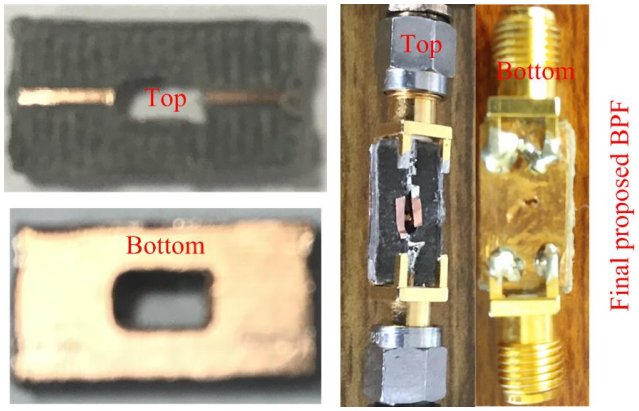

Fig. 6. The fabricated prototype of the proposed DBSO-BPF (with and without connector)

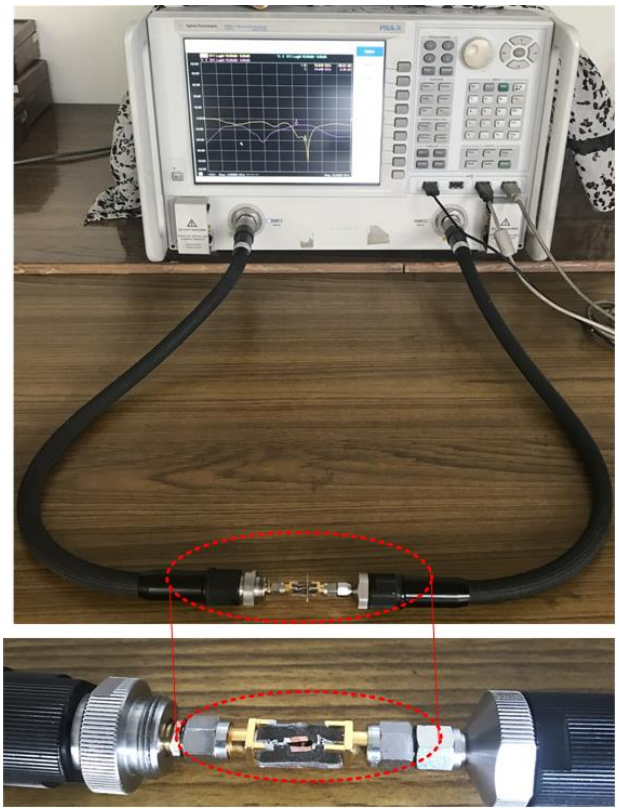

Fig. 7. Measurement setup of the proposed DBSO-BPF with VNA

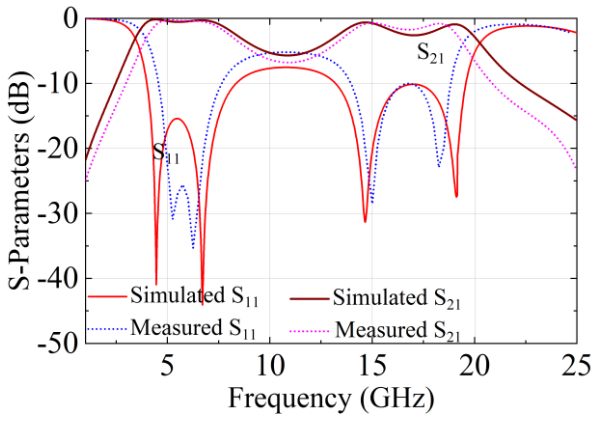

Fig. 8. Simulated and measured S-parameters (magnitude of S_{11} and S_{21}) of DBSO-BFP

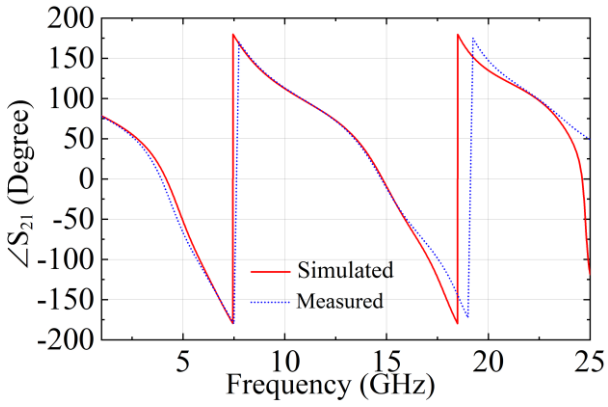

Fig. 9. Simulated and measured of phase of S_{21} (degree) of the DBSO-BPF

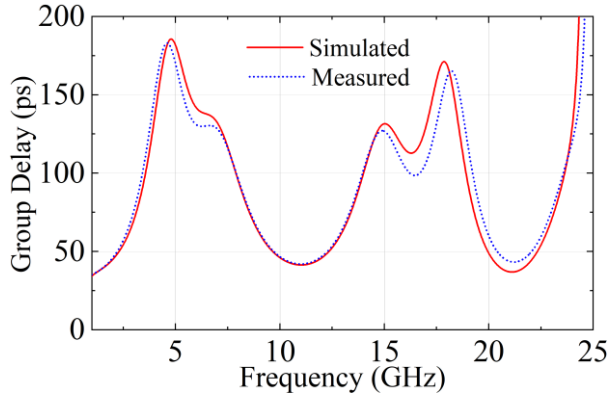

Fig. 10. Simulated and measured group delay (ps) of the DBSO-BPF

The effect of two copper strips or stubs on loss has been reduced using a strongly coupled BPF structure. As a result, two second-order resonators were used to design a C- and Ku-band BPF to demonstrate the aim's viability and approach. The 4 GHz pass-band is centred at 6 GHz and the maximum insertion loss (IL) of 0.32 dB is achieved for the first band while the 6.5 GHz pass-band is centred at 16.25 GHz, and the maximum IL of 0.2 dB is also achieved for the second band. The spurious free bands span approximately from 4-8 GHz for the lower band and the higher band from 13-19.5 GHz are obtained in the proposed work. An appropriate choice of dimension is also necessary for the design because the radiating element and the ground are separated. In order to acquire the broadband operational bandwidth for both bands of the DBSO-BPF configuration, a parametric study (using the full-wave electromagnetic simulator Ansys HFSS 2020R2) about the choosing of the best value for W_g suggests (see Fig. 3) that it should not be larger than the thickness of the substrate (h). Finally, the optimized dimensions of the proposed work are listed below: W_{total}=15 mm, L_{total}=8 mm, L_{feed}=5.25 mm, W_{feed}=0.56 mm, L_1=4.5 mm, W_1=2.8 mm, W_g =0.2 mm, L_{stub}=4.24 mm ($\approx\lambda_g/4$ at mid-band of lower frequency-band, 6 GHz, where λ_g is the guided wavelength), W_{stub}=0.5 mm, t_g=26 mm, W_{gap}=0.8 mm, *and* h=1.524 mm for FR4 (h=1.524 mm for Roger 5880). Fig. 4 shows the electric-field distribution at lower and higher mid-band frequencies of the proposed DBSO-BPF. It is confirmed that the structure propagates the TM mode. In addition, the surface current distribution is also plotted at different frequencies, as shown in Fig. 5.

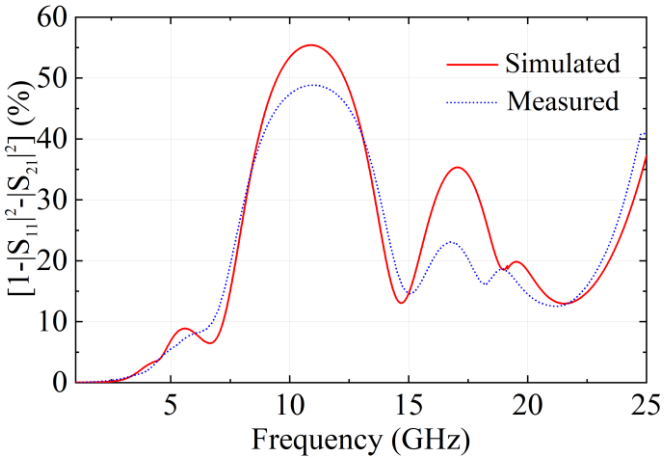

Fig. 11. Simulated and measured total loss (%) of the DBSO-BPF

III. Simulation and Experimental Results

Fig. 6 depicts the fabricated prototype for the top and ground views of the proposed DBSO-BPF (see left side), respectively. The laboratory prototypes with SMA connectors are illustrated in Fig. 6 (see right side). The measurement setup with a vector network analyzer (VNA) and the DBSO-BPF is shown in Fig. 7. The modelling yielded the simulated resonance frequencies of 4.34/7.5 GHz (measured: 5.12/7.02 GHz) for C-band and 14.92/19.18 GHz (measured: 15/18.5 GHz) for the Ku band, which are confirmed through experimentation at those frequencies. On the other hand, Fig. 8 shows the experimental results in conjunction with the S-parameter simulation results. As can be seen from the plot, there are two transmission poles in each band in Fig. 8. As a result, the BPF operates like a dual-band second-order BPF.

TABLE 1
COMPARISON OF THE PROPOSED WORK WITH THE STATE-OF-THE-ART

Ref.	Thickness (λ_0)	f_0 (GHz)	ABW (GHz)	FBW (%)	IL (dB)
[8]	0.017	3.3	0.12	3.7	0.5
[9]	0.005	3.48	0.21	6.28	1.78
[10]	0.054	NR	NR	NR	2.4
[11]	0.003/ 0.008	1.11/ 2.89	0.451/ 0.445	40.41/ 15.36	0.25/ 0.84
[12]	0.009	5.58	0.84	15	0.98
This work	**0.026/ 0.088**	**5.12/ 17.5**	**4/6.5**	**51.64/ 28.48**	**0.64/ 1.02**

FBW: Fractional bandwidth, NR: Not reported, f_0: Resonant frequency

In addition, the simulated absolute bandwidth (ABW) of 4 GHz (4-8 GHz) for the first band and 6.5 GHz (13-9.5 GHz) for the second band is obtained whereas the 3.12 GHz (13.64-16.76 GHz) is the measured ABW. Furthermore, over the whole passband, the minimum simulated and measured insertion loss (IL) of 0.22 and 0.32 dB and the maximum simulated and measured IL of 0.64 and 1.02 dB are achieved.

Additionally, the experimental validation is confirmed using simulation findings of this designed BPF structure, the phase of S_{21}, as illustrated in Fig. 9. This plot shows that the simulated phase of the S_{21} matches precisely. Furthermore, as shown in Fig. 10, the simulated and measured minimal group delays of 0.14 and 0.10 ps are attained within the passband. Conversely, the maximum values of 0.33 and 0.24 ps are found for the simulated and measured group delays, respectively. Furthermore, the total loss is also calculated [18]-[20] in this work, as shown in Fig. 11. The total loss depends on both S_{11} and S_{21}. So, the total loss is $(1-|S_{11}|^2-|S_{21}|^2)$ (in%). The authors have carefully verified both simulation and experimental results. The simulated and measured total loss below 10% is achieved in the range of 4.44–6.7 GHz (lower band). In contrast, the total loss below 30% is achieved in the range of 14.65–19.13 GHz (higher band). Yes, both the simulated and measured total losses are a little bit high due to the fabrication tolerance. Thus, it indicates that the flat group delay and superior linearity of this suggested BPF have improved the filter properties. Finally, a comparison table is included in order to compare with the previous work, as shown in Table I. It can be observed in Table I that the FBW and ABW are higher than the reported work [8]–[12]. However, the IL is a little bit higher than [8] and [11] and better than [9], [10], and [12].

IV. Conclusion

The dual-band second-order BPF, which addresses the compact size and achieves a broader bandwidth, is covered in the proposed work. It employs a straightforward strategy in conjunction with aperture coupling approaches. On the other hand, the structure is designed, simulated, fabricated, and experimentally validated of filter properties, and it is cross-checked with all experimental results. These findings are consistent with one another. The measured fractional IBW of the planner DBSO-BPF achieved at the first and second resonant frequencies, respectively, is 51.67 and 28.43 %. Throughout the bandwidth, the minimum measured IL is less than 0.64, and 1.02 dB (simulated: 0.22 and 0.32 dB) are achieved. The proposed DBSO-BPF can be used for various wireless services, radar, and satellite communication applications in C-and Ku-band applications.

Acknowledgement

RM would now take this opportunity to express gratitude to BPPIMT'S authorities for providing the scope to pursue my Ph.D. work at GIET University and the required support. We also thank all reviewer for their comments on the potential of our manuscript. We also thank Mr. S. Gaur for their assistance in fabricating this work.

References

[1] M. Uhm, K. Ahn, I. Yom and J. Kim, "A Triple-Passband Waveguide Filter with Dual-Mode Resonators for Ka Band Satellite Applications," in *24th AIAA International Communications Satellite Systems Conference* , June 2006.

[2] S. Bastioli, C. Tomassoni and R. Sorrentino, "A New Class of Waveguide Dual-Mode Filters Using TM and Nonresonating Modes," in *IEEE Trans. Microwave Theory and Techniques*, vol. 58, no. 12, pp. 3909-3917, Dec. 2010.

[3] U. Rosenberg, S. Amari and J. Bornemann, "Inline TM/Sub 110/-Mode Filters with High-Design Flexibility by Utilizing Bypass Couplings of Nonresonating TE/Sub 10/01/ Modes,"

in *IEEE Trans. Microwave Theory and Techniques*, vol. 51, no. 6, pp. 1735-1742, June 2003.

[4] S. Bastioli, C. Tomassoni, and R. Sorrentino, "TM Dual-Mode Pseudoelliptic Filters Using Nonresonating Modes," in *IEEE MTT-S International Microwave Symposium*, pp. 880-883, 2010.

[5] S. Bastioli, L. Marcaccioli, C. Tomassoni, and R. Sorrentino, "Ultracompact Highly-Selective Dual-Mode Pseudoelliptic Filters," *IET Electronics Letters*, vol. 46, no. 2, pp. 147–149, 2010.

[6] C. Tomassoni, S. Bastioli and R. Sorrentino, "Generalized TM Dual-Mode Cavity Filters," in *IEEE Transactions on Microwave Theory and Techniques*, vol. 59, no. 12, pp. 3338-3346, Dec. 2011.

[7] L. Pelliccia, F. Cacciamani, C. Tomassoni, and R. Sorrentino "Ultra-Compact High-Performance Filters Based on TM Dual-Mode Dielectric-Loaded Cavities" *International Journal of Microwave and Wireless Technologies*, vol. 6, no. 2, pp. 151-159, Apr. 2014.

[8] W. Afzal, A. Ebrahimi, M. R. Robel and W. S. T. Rowe, "Low-Profile Higher-Order Narrowband Bandpass Miniaturized-Element Frequency-Selective Surface," in *IEEE Transactions on Antennas and Propagation*, vol. 71, no. 4, pp. 3736-3740, April 2023.

[9] Y. Wu, K. Ma, S. Li and Y. Zhan, "Design of Vertically Integrated Folded SISL Patch Bandpass Filters With Single and Multiband Responses," in *IEEE Transactions on Components, Packaging and Manufacturing Technology*, vol. 14, no. 3, pp. 479-488, March 2024.

[10] P. N. Choubey and W. Hong, "Dual-Band Bandpass Filter Designed by Exploiting the Second-Order Degenerated Modes of the SIW-Cavity," *Asia-Pacific Microwave Conference (APMC)*, pp. 1-3, 2015.

[11] L. Yang, M. Malki and R. Gómez-García, "Multilayer Dual-Band Bandpass Filter Using Microstrip-to-Slotline Transitions and Transversal Signal-Interference Microstrip Lines," *2024 IEEE Radio and Wireless Symposium (RWS)*, pp. 79-82, 2024.

[12] P. Pech, S. Saron, G. Chaudhary and Y. Jeong, "Ultra-Compact Substrate Integrated Waveguide Bandpass Filter with Unequal Termination Impedance," *Asia-Pacific Microwave Conference (APMC)*, pp. 134-136, 2023.

[13] F. Arndt, T. Duschak, U. Papziner, and P. Roalppe, "Asymmetric Iris Coupled Cavity Filters with Stopband Poles", in *IEEE International Digest on Microwave Symposium*, pp. 215–218, 1990.

[14] M. Guglielmi, F. Montauti, L. Pellegrini, and P. Arcioni, "Implementing Transmission Zeros in the Inductive-Window Bandpass Filters", in *IEEE Transactions on Microwave Theory and Techniques*, vol. 43, no. 8, pp. 1911–1915, Aug. 1995.

[15] C. Tomassoni *et al*., "Compact Broadband Waveguide Filter with Wide Spurious-Free Range Based on Mixed TM and Combline Resonators," *47th European Microwave Conference (EuMC)*, pp. 985-988, 2017.

[16] L. Pelliccia *et al*., "Very-compact Waveguide Bandpass Filter based on Dual-Mode TM Cavities for Satellite Applications in Ku-band," *48th European Microwave Conference (EuMC)*, pp. 93-96, 2018.

[17] L. Pelliccia, F. Cacciamani, P. Vallerotonda, C. Tomassoni and R. Sorrentino, "Miniaturization High-Performance Bandpass Filters for Satellite Applications,"in *IEEE MTT-S International Microwave Workshop Series on Advanced Materials and Processes for RF and THz Applications (IMWS-AMP)*, pp. 1-3, 2017.

[18] A. K. Navak, I. M. Filanovsky, K. Moez and A. Patnaik, "Broadband Conductor Backed-CPW With Substrate-Integrated Coaxial Line to SIW Transition for C-Band," in *IEEE Transactions on Circuits and Systems II: Express Briefs*, vol. 69, no. 5, pp. 2488-2492, May 2022.

[19] A. A. Khan and M. K. Mandal, "A Compact Broadband Direct Coaxial Line to SIW Transition," in *IEEE Microwave and Wireless Components Letters*, vol. 26, no. 11, pp. 894-896, Nov. 2016.

[20] A. K. Navak, I. M. Filanovsky, K. Moez and A. Patnaik, "Broadband Conductor Backed-CPW with Tapered Microstrip Line to Corrugated Via Wall-SIW Transition for Different-Bands (2–40 GHz),"in *IEEE International Symposium on Circuits and Systems (ISCAS)*, pp. 1-5, 2023.